SCIENTIFIC REPORTS

OPEN

Tunable Ampere phase plate for low dose imaging of biomolecular complexes

Amir H. Tavabi [1], Marco Beleggia[2], Vadim Migunov [1], Alexey Savenko[3], Ozan Öktem[4], Rafal E. Dunin-Borkowski[1] & Giulio Pozzi[1,5]

A novel device that can be used as a tunable support-free phase plate for transmission electron microscopy of weakly scattering specimens is described. The device relies on the generation of a controlled phase shift by the magnetic field of a segment of current-carrying wire that is oriented parallel or antiparallel to the electron beam. The validity of the concept is established using both experimental electron holographic measurements and a theoretical model based on Ampere's law. Computer simulations are used to illustrate the resulting contrast enhancement for studies of biological cells and macromolecules.

The imaging of biomolecular complexes with near-atomic spatial resolution is crucial for our understanding of how biological functions emerge from a set of building blocks that are carefully orchestrated by the laws of physics and chemistry. Aberration correction in transmission electron microscopy (TEM) now provides sub-Ångström point resolution at low and medium (20–300 kV) accelerating voltages[1–3]. When accompanied by the latest generation of electron detectors, these instruments provide an almost ideal platform for addressing outstanding problems in structural biology. However, one issue remains: biological structures interact with an incoming high-energy electron beam by modulating the phase of the electron wave very weakly. A "phase-sensitive" imaging method is then required to turn an invisible phase modulation into visible contrast that can be recorded, analyzed and linked back to the number, positions and species of atoms present.

In-focus phase contrast devices[4,5] that are analogues of the optical phase plate (PP) introduced by Zernike[6] have been investigated for decades and emerged from a wide range of possible phase-sensitive imaging techniques as promising and viable methods for enhancing the contrast of biological specimens in the TEM. However, according to Glaeser[5], most PPs that have been proposed so far suffer from deficiencies that include insufficient contrast enhancement, additional aberrations, short lifetimes, a lack of a straightforward alignment method and/or electrostatic charging by the electron beam (even when self-charging is responsible for producing phase contrast)[7,8]. In particular, charging is very difficult to measure and control, deteriorates device performance and limits widespread applications.

Here, we introduce a new substrate-free PP concept for TEM that is based on Ampere's law and addresses all of these problems. We refer to the device as a "tunable Ampere phase plate" (TAPP). It is designed to provide almost-ideal phase contrast, while maintaining 1–4 Å spatial resolution and providing both tunability and ease of application.

The functionality of the TAPP is provided by a magnetic field circulating around a vertical segment of current-carrying wire, which adds a position-dependent phase shift to a passing electron wave. When the TAPP is positioned in the back focal plane of the imaging lens, it acts as an additional transfer function that enhances phase contrast from the object.

We used focused ion beam (FIB) milling to fabricate a prototype TAPP from etched Au wires in the form of three orthogonal segments, thereby making a hook-shaped device, as shown in Fig. 1a. One segment of the hook could then be positioned parallel and the other two perpendicular to the incident electron beam direction. In the present study, the device was mounted in the specimen plane in order to measure its phase shift. The geometry of

[1]Ernst Ruska-Centre for Microscopy and Spectroscopy with Electrons and Peter Grünberg Institute, Forschungszentrum Jülich, 52428, Jülich, Germany. [2]Center for Electron Nanoscopy, Technical University of Denmark, 2800, Kgs Lyngby, Denmark. [3]FEI Company, Achtseweg Noord 5, 5600 KA, Eindhoven, The Netherlands. [4]Centre for Industrial and Applied Mathematics, Department of Mathematics, KTH - Royal Institute of Technology, Stockholm, Sweden. [5]Department of Physics and Astronomy, University of Bologna, Viale B. Pichat 6/2, 40127, Bologna, Italy. Correspondence and requests for materials should be addressed to A.H.T. (email: a.tavabi@fz-juelich.de)
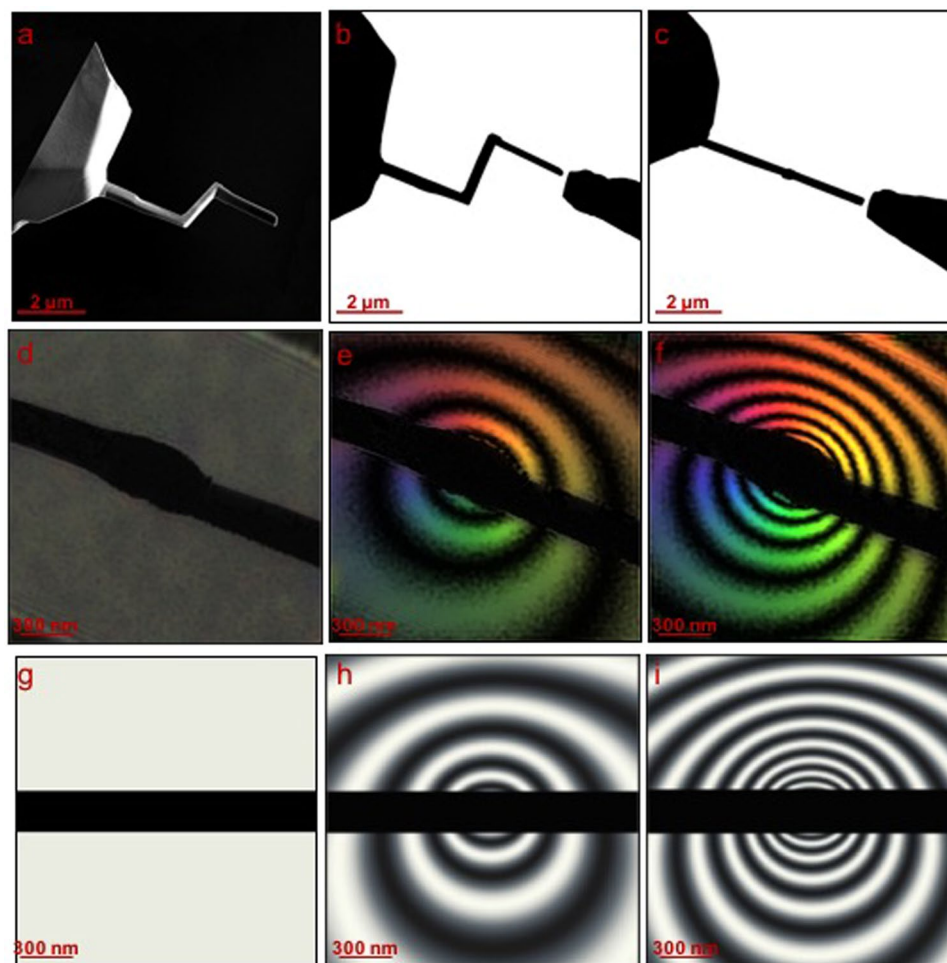
Figure 1. (**a**) Secondary electron image of the TAPP device recorded before connecting it to a counter-electrode. (**b,c**) Bright-field images of the device viewed in the specimen plane in a TEM at tilt angles of 70° and 0° with respect to the optic axis of the microscope, respectively. The counter-electrode, which is movable in the present setup, is visible on the right of each image. (**d–f**) 8× amplified phase images of the vacuum region around the phase plate recorded using off-axis electron holography for currents through the device of (**d**) 0, (**e**) 2 and (**f**) 4 mA. (**g–i**) Simulated 8× amplified phase images for currents of (**g**) 0, (**h**) 2 and (**i**) 4 mA, including the influence of the perturbed reference wave.

the wire is shown in Fig. 1b,c, viewed at tilt angles of 70° and 0° with respect to the incident electron beam direction, respectively. The wire was connected electrically inside the TEM using a nanopositioning specimen holder (Fig. S1), closing the circuit and allowing a current to flow (Fig. S2). The phase shift introduced by the TAPP was recorded directly using off-axis electron holography, with the short segment of the hook oriented parallel to the electron beam direction, for varying currents[9] and compared with a theoretical model based on Ampere's law. A schematic diagram of the experimental setup is shown in Fig. S3.

Figure 1d–f show maps of the phase shift introduced by the TAPP measured using off-axis electron holography. A representative original electron hologram is shown in Fig. S4. The maps are displayed in the form of 8× amplified phase contours (generated using the expression $1 + \cos[8 \times \text{phase}(x, y)]$), in order to provide a visual illustration of the projected in-plane magnetic field distribution surrounding the object. The tilted bar in each image is the shadow of the horizontal segments of the hook, which are opaque to electrons, while the wider region at its center corresponds to the position of the vertical segment of the wire. Figure 1d shows a phase image recorded using electron holography in the absence of current flow. The signal is essentially flat, with only Fresnel fringes caused by the edges of the biprism wire that was used to form the hologram visible at the edge of the field of view, indicating that neither magnetic nor electrostatic fields are present around the device. Although this conclusion is at first sight expected as there is no current flowing, its experimental verification is important as it demonstrates that there is no unwanted electron beam induced charging when the phase plate is operated inside the microscope. It is also important to note that electron beam induced charging is unlikely due to the metallic nature of the device, coupled with heating from the current flow. However, should it arise, it can be compensated simply by varying the current in the device, as a result of the electron optical equivalence between the phase shift arising from an electrical charge and from a vertical current segment, as discussed in the Supplementary Material.
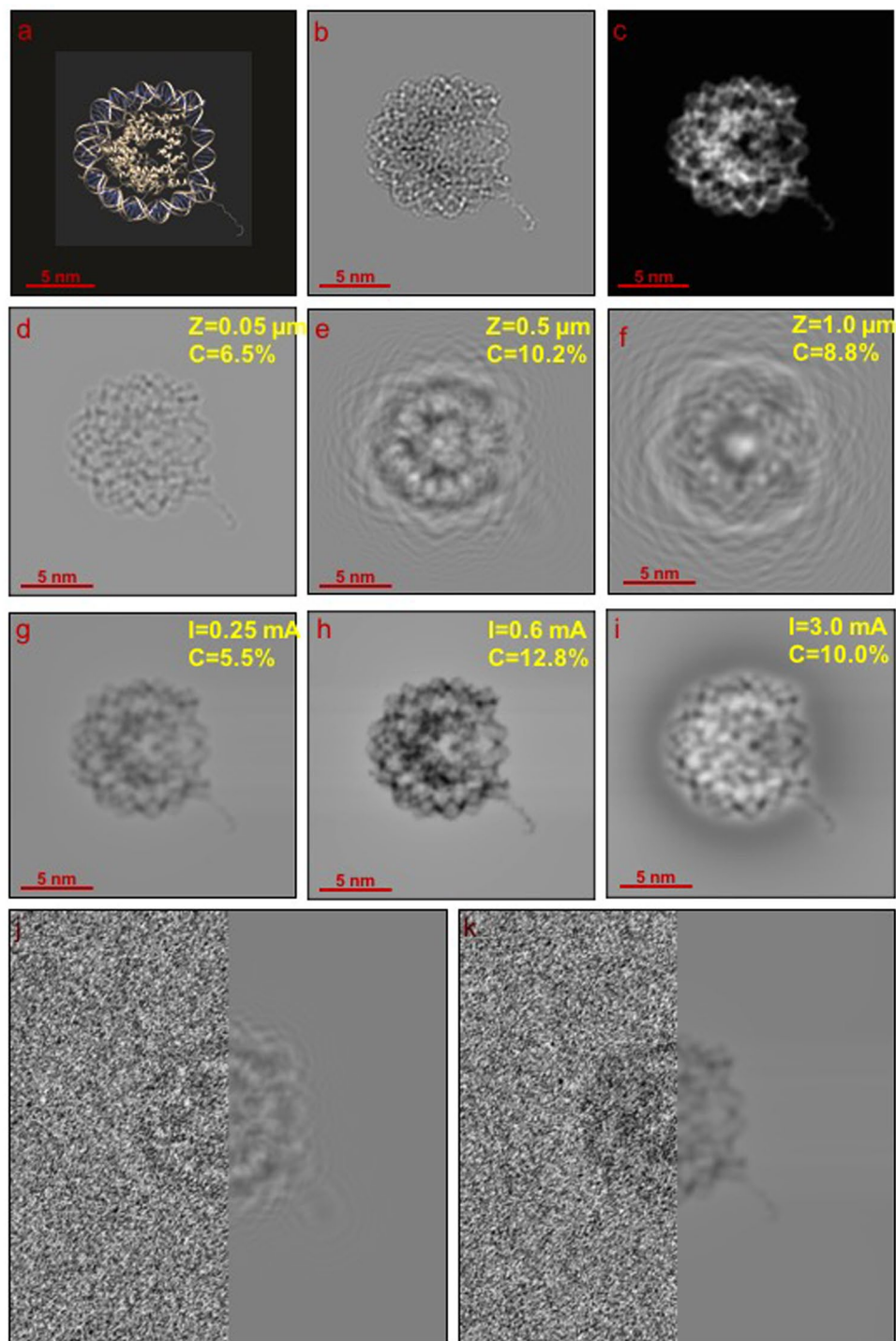
Figure 2. (**a**)Molecular structure of the NCP. (**b**) Amplitude and (**c**) phase of the electron wave transmitted by the NCP at 200 kV; the images are density-plotted over their full ranges: 0.770–0.790 for the amplitude and 1.59–1.71 rad for the phase. (**d**–**f**) Simulated out-of-focus Fresnel images for defocus values of (**d**) 0.05, (**e**) 0.5 and (**f**) 1.0 μm. (**g**–**i**) Simulated TAPP images for currents of (**g**) 0.2, (**h**) 0.6 and (**i**) 3.0 mA. The image contrast $C = (I_{max} - I_{min})/(I_{max} + I_{min})$ is specified at the top right corner of each simulation. (**j**) and (**k**) show how typical levels of noise would affect the object visibility for the out-of-focus and TAPP images.

Together with its tunability, this is one the most advantageous aspects of the TAPP when compared with most other phase plate concepts, as it resolves the most prominent limiting factor of uncontrolled charging, which has previously prevented widespread phase plate applications. Figure 1e shows a phase image recorded when a nominal current of 2 mA is passed through the device. The rings represent projected in-plane magnetic field lines. Colors are used to represent the direction of the projected in-plane magnetic field. The lack of circular symmetry results from the use of a perturbed reference wave when acquiring off-axis electron holograms in the presence

of a long-range magnetic field[10]. However, this effect does not influence the practical operation of the TAPP as a phase plate because, when it is placed in a focal plane, the phase shift that it adds to scattered electrons is not influenced by a perturbed reference wave. In accordance with Ampere's law, increasing the current two-fold to 4 mA (Fig. 1f) yields twice the phase shift. A comparison between Fig. 1e,f reveals that at every point the magnitude of the signal is doubled, while maintaining an identical decay with distance, as shown in the form of phase shift profiles in Fig. S5.

Figure 1g–i show corresponding calculated phase images, also displayed as 8× amplified contour maps, for a vertical current segment that has a length of 2 μm and for current flows of 0, 2 and 4 mA in Fig. 1g–i, respectively. The black bar mimics the opaque projection of the device. The consistency between the simulated and experimental images confirms that the TAPP functions as an electron phase shifting device that is easily tunable.

In order to assess the performance of the TAPP in the back focal plane of the microscope, we carried out simulations for a nucleosome core particle (NCP), PDB-ID: 1AOI, whose molecular structure is shown in Fig. 2a [11]. The simulations mimic a realistic experimental setup, with the NCP virtually embedded in a 50-nm-thick layer of water ice and imaged at an accelerating voltage of 200 kV. Figure 2b,c show the amplitude and phase of the electron wave transmitted through the NCP, respectively, calculated using the approach described in ref[12]. The simulated amplitude image, which varies locally by only 2.5%, reveals that the NCP does not contribute substantially to the effective absorption of the ice embedment, which removes as much as 40% of the incoming electrons. In contrast, the phase image is more directly related to the local projected atomic/molecular weight of the NCP and reveals a relatively strong phase shift between the ice (1.59 rad at 200 kV for a 50-nm-thick ice layer with a mean inner potential of 4.4 V) and the interior of the NCP (1.71 rad maximum), reflecting the presence of elements that are heavier than oxygen, as well as denser regions. Comparing Fig. 2a with Fig. 2b,c visually, a resemblance is recognized more easily with the phase image, indicating that, as expected, structural information is encoded more directly in the phase of the electron wave than in its amplitude.

In comparison, Fig. 2d–f show simulated Fresnel defocus images calculated in the absence of noise and aberrations, illustrating how the conventional out-of-focus technique blurs information when a defocus value that is large enough to provide sufficient contrast is used. At a defocus of 0.05 μm, the contrast in Fig. 2d is very low and the image resembles more the amplitude in Fig. 2b than the phase in Fig. 2c. When the defocus is set to 0.5 μm (Fig. 2e), the contrast increases to approximately 10% and some phase information is visible, but the structural details are now blurred. An increase in defocus to 1.0 μm (Fig. 2f) provides no further advantages, as the contrast decreases and the details are washed out. Although it is possible to correct for contrast reversal and damping due to the contrast transfer function (CTF), there are two disadvantages to applying CTF correction to a single defocused image, even for a pure phase object: first, it is not possible to retrieve the spatial frequencies at transfer gaps (at the lowest spatial frequencies and at zero crossings in an oscillating CTF) and, second, it is not possible to correct for delocalization resulting from the applied defocus. The use of a series of defocused images with different CTFs is usually precluded for biomolecular imaging due to the higher rate of sample damage.

Figure 2g–i show image simulations for the TAPP device, revealing a clear and recognizable phase contrast image with high contrast of approximately 12% when a current of 0.60 mA is applied (Fig. 2h). Such an image cannot be achieved using the out-of-focus technique. At lower current values, for example 0.25 mA (Fig. 2g), phase contrast is preserved but the contrast is lower. An increase in the current to 3 mA results in a contrast reversal of the NCP, which now appears brighter than the background (Fig. 2i), as well as mixing phase and amplitude information and adding a surrounding halo. The "tail" of the NCP (marked by a red arrow in Fig. 2a,c) remains well-defined in all of the TAPP simulations, indicating that 2–3 Å spatial resolution can be preserved even at relatively large current values. In contrast, when using the out-of-focus technique, the tail disappears as soon as the defocus is high enough to provide sufficient contrast.

During operation, the TAPP is placed in the back focal plane of the imaging lens beside the unscattered beam at $q = 0$, resulting in a slight asymmetry between the phase shift added to electrons at $+q$ and $-q$ along the offset direction (whereas no phase difference arises along the perpendicular direction). This asymmetry results in a small degree of astigmatism. However, the tunability of the TAPP allows any desired phase shift to be chosen between the scattered and unscattered beams in Fraunhofer space (see Fig. S7).

In summary, we have introduced a new substrate-free phase plate, which is based on Ampere's law and offers significant advantages over previous designs. It provides tunability, radial phase shifting homogeneity, minimal aberrations, almost no delocalization, ease of operation, almost-ideal phase contrast (where ideal phase contrast means that the image intensity is linearly proportional to the phase shift) for a weak phase object and a simplified fabrication procedure. In contrast to other proposals for phase plates based on magnetic fields, it does not rely on the presence of ferromagnetic material and can therefore be used in the strong objective lens field of the electron microscope. The implementation of a TAPP in a modern cryo electron microscope promises to contribute to the advancement of structural biology, ultimately in combination with spherical and chromatic aberration correction and electron tomography, to achieve 1–2 Å spatial resolution and the full three-dimensional atomic structure of complex biomolecules.

References

1. Danev, R. & Baumeister, W. Cryo-EM single particle analysis with the Volta phase plate. *eLife.* **5**, e13046 (2016).
2. Khoshouei, M. *et al.* Volta phase plate cryo-EM of the small protein complex Prx3. *Nat. Commun.* **7**, 10534 (2016).
3. Chua, E. Y. D. *et al.* 3.9 Å structure of the nucleosome core particle determined by phase-plate cryo-EM. *Nucleic Acids Res.* **44**, 8013–8019 (2016).
4. Nagayama, K. Another 60 years in electron microscopy: development of phase-plate electron microscopy and biological applications. *J. Electron Microsc.* **60**, S43–S62 (2011).
5. Gleaser, R. M. Invited Review Article: Methods for imaging weak-phase objects in electron microscopy. *Rev. Sci. Instrum.* **84**, 111101 (2013).
6. Zernike, F. Phase contrast, a new method for the microscopic observation of transparent objects. *Physica* **9**, 686–698 (1942).

7. Danev, R., Buijsse, B., Khoshouei, M., Plitzko, J. M. & Baumeister, W. Volta potential phase plate for in-focus phase contrast transmission electron microscopy. *P. Natl. Acad. Sci. USA* **111**, 15635–15640 (2014).
8. Malac, M., Beleggia, M., Kawasaki, M., Li, P. & Egerton, R. F. Convenient contrast enhancement by a hole-free phase plate. *Ultramicroscopy* **118**, 77–89 (2012).
9. Pozzi, G., Beleggia, M., Kasama, T. & Dunin-Borkowski, R. E. Interferometric methods for mapping static electric and magnetic fields. *Comptes Rendus Physique* **15**, 126–139 (2014).
10. Matteucci, G., Missiroli, G. F. & Pozzi, G. *Advances in Imaging and Electron Physics*, pp. 173–249, (Elsevier, 2002).
11. Luger, K., Mäder, A. W., Richmond, R. K., Sargent, D. F. & Richmond, T. J. Crystal structure of the nucleosome core particle at 2.8 Å resolution. *Nature* **389**, 251–260 (1997).
12. Rullgård, H., Öfverstedt, L. G., Masich, S., Daneholt, B. & Öktem, O. Simulation of transmission electron microscope images of biological specimens. *J. Microsc.* **243**, 234–256 (2011).

Acknowledgements

Author Contributions

A.H.T., V.M., R.E.D.-B. and G.P. conceived the idea; A.S. fabricated the device; A.H.T. and V.M. performed the experiments; A.H.T., V.M. and R.E.D.-B. analyzed the data; G.P. and M.B. developed the theoretical framework; O.Ö. calculated the phase shift of the NCP molecular structure; M.B. performed image simulations for the NCP; all of the authors discussed the results and contributed to the text of the manuscript.

Additional Information

Supplementary information accompanies this paper at https://doi.org/10.1038/s41598-018-23100-3.

Competing Interests: The authors declare no competing interests.

Publisher's note: Springer Nature remains neutral with regard to jurisdictional claims in published maps and institutional affiliations.